

PRODUCTION AND CHARACTERIZATION OF Al-xNi IN SITU COMPOSITES USING HOT PRESSING

R. Yamanoglu *

Department of Metallurgical and Materials Engineering, Kocaeli University, Umuttepe Campus, Kocaeli 41380, Turkey

(Received 17 July 2013; accepted 02 December 2013)

Abstract

In this study, a new metal matrix composite of aluminium was designed with the addition of nickel alloy particles. To produce in situ intermetallic formation, aluminium-nickel powder mixtures with different ratios ranging from 5 to 40 wt% Ni were consolidated at 550 °C for 15 minutes under 40 MPa pressure. The interlayer phase formed during sintering was determined using X-ray diffraction and energy dispersive X-ray spectroscopy. The effect of nickel and Al-Ni intermetallics on the mechanical properties of the material was studied. The results demonstrated that the addition of nickel enhanced the hardness and wear behaviour of aluminium by forming a strong bonding interface between the aluminium and nickel particles.

Keywords: Aluminium, nickel, hot pressing, in-situ composite

1. Introduction

Recently, many studies have focused on enhancing the properties of aluminium alloys due to the weak mechanical properties of pure aluminium. Alloying of aluminium with different elements has attracted the attention of many researchers [1-5]. By means of alloying over the past two decades, researchers have shown a growing interest in intermetallics that are comprised of two or more metallic elements with specific stoichiometries and that have high mechanical and temperature properties. Ti-Al, Ni-Al and Fe-Al alloys are the most often used intermetallics for technological applications [6-7]. These intermetallics are stronger, stiffer and more corrosion resistant at high temperatures. These properties make them suitable for improving the performance of engines, pumps, vehicles, heat exchangers, tools and die parts [8]. One of the most promising alloying elements to enhance the mechanical properties of pure aluminium is nickel. Because of the low solubility of nickel in aluminium, five intermetallic compounds can exist in the Al-Ni binary system: Al₃Ni, Al₃Ni₂, AlNi, Al₃Ni₅ and AlNi₃ [9]. A number of studies have indicated that nickel aluminides have significant potential in wear-critical applications [10].

Previous studies have reported the formation of

aluminium intermetallic compounds by using different techniques such as mechanical alloying (MA) [11], combustion synthesis (CS), reaction synthesis (RS) [12] and casting techniques [13], resulting in improved mechanical and chemical properties. Ikenaga showed that Ni-Al based intermetallics could be synthesised directly from the mixture of Al and Ni powders [14-15]. The fabrication of Ni_xAl_y intermetallics by conventional casting techniques is difficult and costly for processing structural parts. Powder metallurgy is a good technique for producing materials with better mechanical properties. By means of hot pressing, it is easy to control the intermetallic formation between alloying elements. Recently, there have been many studies that have been focused on the behaviour of conventionally cast Ni_xAl_y alloys, but few studies have been carried out on powder metallurgical materials consolidated by hot pressing [16-17]. Furthermore, most of the PM methods used mechanically alloyed powders. In the current study, intermetallic compounds were produced during hot pressing.

In this study, a metal matrix composite including in situ Ni-Al intermetallic formation was successfully produced by hot pressing. The effect of nickel content was investigated by X-ray diffraction, SEM, hardness tests and metallographic examinations.

* Corresponding author: ryamanoglu@kocaeli.edu.tr

2. Experimental

Commercially available 99.8% pure Al powder with an average particle size of 69 μm and a reinforcement nickel alloy powder ($_{1.25}\text{Al-}_{6.22}\text{Si-}_{1.58}\text{P-}_{2.96}\text{Cr-}_{1.10}\text{Fe-}_{\text{remainder}}\text{Ni}$ (wt%), $\approx 45 \mu\text{m}$) were provided by Sentes-BIR A. S. (Izmir, Turkey) and used as the starting materials. SEM images of the powders are shown in Figure 1. To produce composite samples, aluminium and nickel alloy powders with different nickel ratios (5-40 wt%) were mixed mechanically and then poured into graphite dies coated with boron nitride.

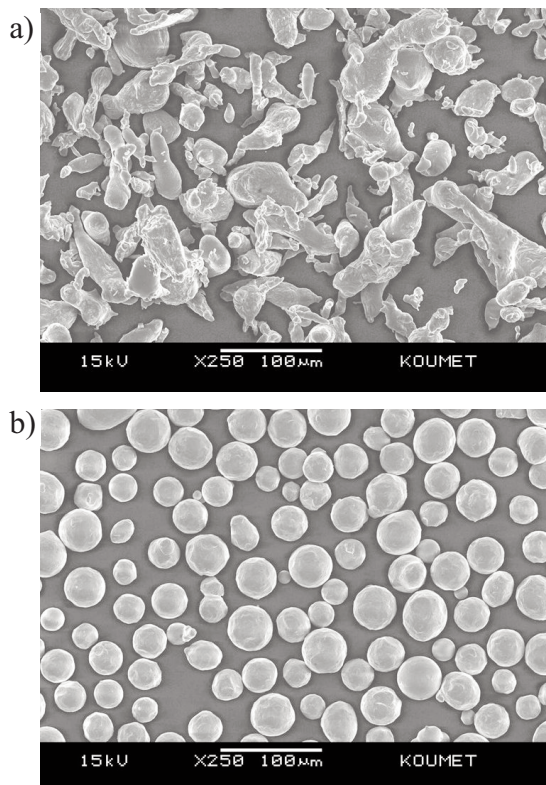


Figure 1. SEM images of powders used in this study, a) Al and b) Ni powder

The Al-Ni powder mixtures were consolidated by uniaxial vacuum hot pressing at 550 $^{\circ}\text{C}$ for 15 minutes with a 20 $^{\circ}\text{C min}^{-1}$ heating rate under 40 MPa pressure in a graphite die set having a 20 mm interior diameter. Pure aluminium compacts exhibited 98.2% of relative density using these processing parameters. The hot-pressing process was accomplished using a DIEX VS 50 automatic sintering machine (DIEX Corp.). A schematic illustration of the process and sintering cycle is shown in Figure 2. During the soaking time of 15 min, the temperature was monitored by an infrared pyrometer. To determine the effect of nickel on the hardness and wear properties of the material, the hot-pressing parameters were fixed and the nickel ratios were changed.

The microstructural characterisation was conducted using an optical microscope (OM) and a scanning electron microscope equipped with an energy dispersive X-ray spectrometer. The specimens for OM and SEM were prepared by the standard technique of grinding and polishing. To understand the effect of nickel on the mechanical properties, hardness and wear tests were performed. Vickers hardness tests were performed using a Future-Tech-type Vickers hardness tester under 3 kg load and 10 seconds of loading duration. All of the reported hardness values are based on the average of five measurements. To show the effect of nickel content on the tribological properties of the alloy, wear tests were employed at room temperature under dry sliding conditions.

A Nanovea MT/60/NI-type pin-on-disc tribometer (Figure 3), which permits rotation of a flat specimen against a stationary pin or ball, was used in the wear tests. All of the wear tests were carried out under 20 N normal load using AISI 52100 steel balls (5 mm in diameter) as the counterface. The sliding speed and sliding distance were kept constant at 0.13 m/s and 500 m, respectively, for all tests. During the wear tests, the friction coefficients were recorded continuously. The specimens were thoroughly cleaned with alcohol after the wear tests, and then dried with a hot-air blower. The weight loss of the alloys was

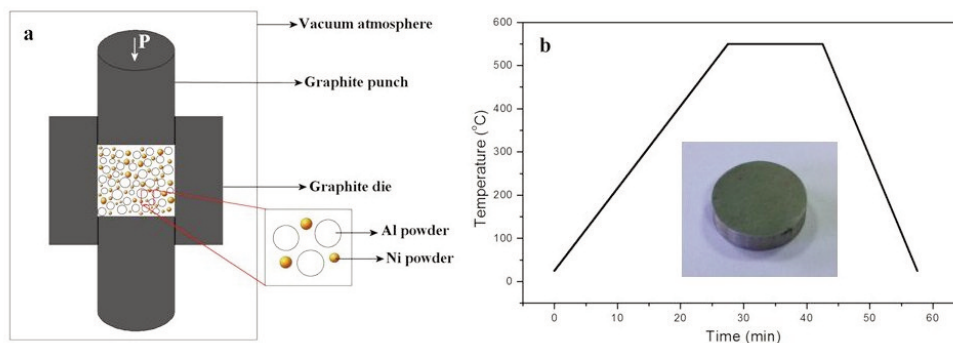


Figure 2. Schematic of hot press process (a) and sintering cycle at 550 $^{\circ}\text{C}$ for 15 min (b)

measured using an AND GR200-type microbalance with a resolution of 0.1 mg. The following equation was used to obtain the wear rate of the specimens: $W = M/\rho D$, where W is the wear rate (mm^3/m), M denotes mass loss (g), and ρ (g/mm^3) and D (m) are the density and sliding distance, respectively [18]. The worn surfaces of the specimens after the wear tests were also investigated using scanning electron microscopy (JEOL JSM 6060) and EDS.

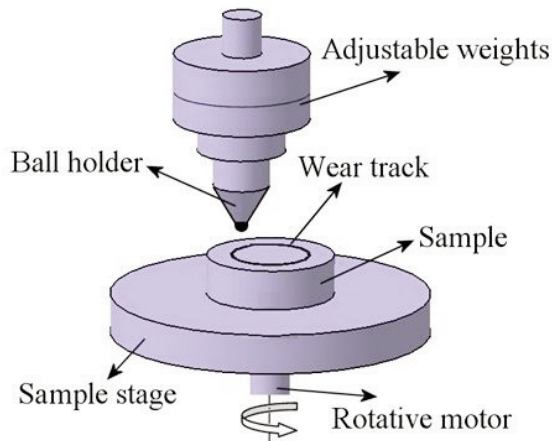


Figure 3. A schematic illustration of wear test device

3. Results and Discussion

Figure 4 shows the polished microstructure images of the sintered Al-Ni compacts by means of optical microscopy. Metallographic sections revealed that the samples contained a mixture of an aluminium matrix, nickel reinforcement particles and an interface layer, as depicted in Figure 5. As can be seen in the figure, the structure indicates that the nickel particles have a homogenous distribution in the aluminium matrix. There is a diffusion reaction between the aluminium and nickel particles during sintering, leading to strong interfacial bonding. This bonding layer is vital for composite materials because the mechanical properties of the composite materials are enhanced and characterised by this bonding mechanism [19].

The microstructure details at higher magnification in Figure 5a-b also demonstrate that there is a well-bonded interface between the aluminium matrix and nickel particles. This bonding structure consists of Ni_xAl_y intermetallics and provides higher mechanical properties to the aluminium. Large nickel particles are uniformly coated with a thin intermetallic layer, whereas most of the small nickel particles were consumed completely and converted into intermetallics, as shown in Figure 5a. A schematic sketch of this bonding mechanism is given in Figure 5c.

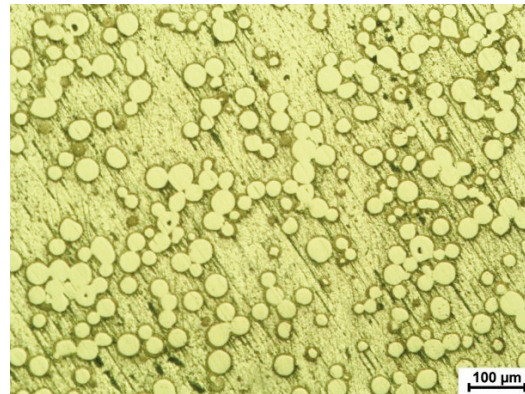


Figure 4. Typical micrograph of the sintered compacts fabricated in this study

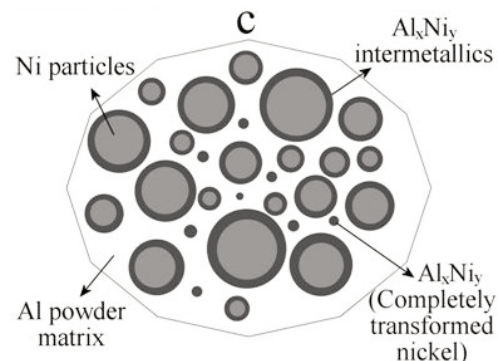
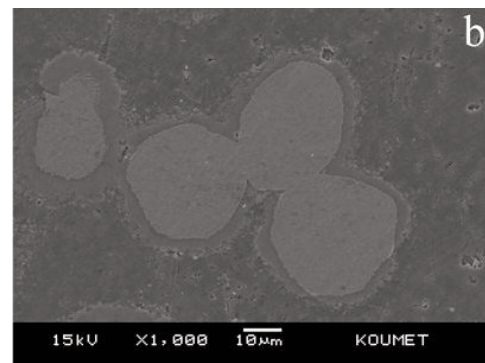
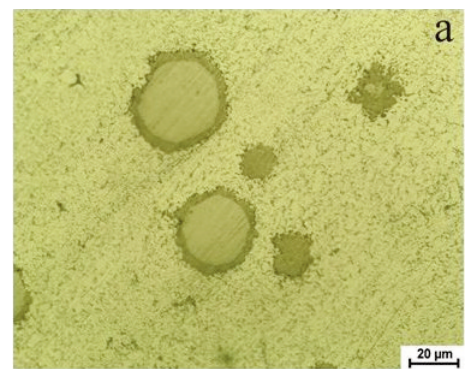


Figure 5. Microstructure of Al/Ni composite like structure a) Optical, b) SEM microscopy and c) schematic representative of composite structure

X-ray diffraction and EDS analysis studies of the sintered compacts were conducted to determine the composition of the bonding layer formed during consolidation. Figure 6 shows the XRD pattern evolution of the sintered compacts. Ni_3Al and Ni_5Al_3 intermetallics identified by XRD were formed in situ during sintering. The diffraction of the other compounds was too weak to be detected.

In addition to the XRD results, according to the EDS analysis on the sintered samples, the results indicate that the interlayer is composed of Al and Ni. The results for the reinforcement particles and matrix are also given in Figure 7. It can be concluded that the reactive area forms intermetallic compounds of Ni and Al.

The mechanical properties of the sintered compacts were studied after determining the phases. Figure 8 shows the hardness (average of five tests) of the sintered compacts as a function of the nickel content. As expected, the hardness increased with increasing nickel and intermetallic content. It is seen from the figure that the hardness increased gradually at the beginning due to the large soft matrix area and then considerably increased above 20 wt% Ni content.

The increase of hardness enhanced the tribological properties of the composite material. The dry sliding wear test results of the alloy shows that the wear rate initially decreases significantly with increasing nickel content then tends to decrease slightly, reaching a minimum value at 25 wt-% Ni before starting to increase (Figure 9).

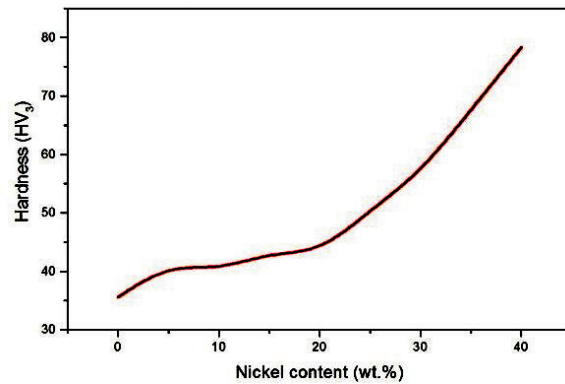


Figure 8. Hardness versus nickel content

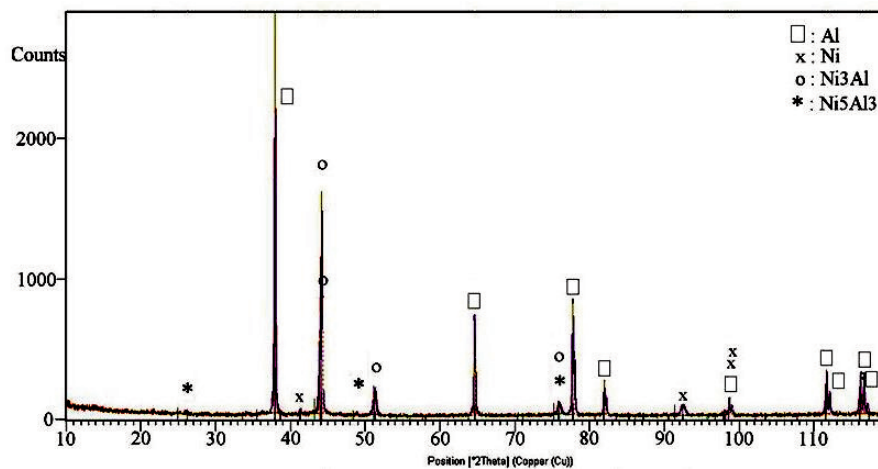


Figure 6. The XRD patterns of sintered sample

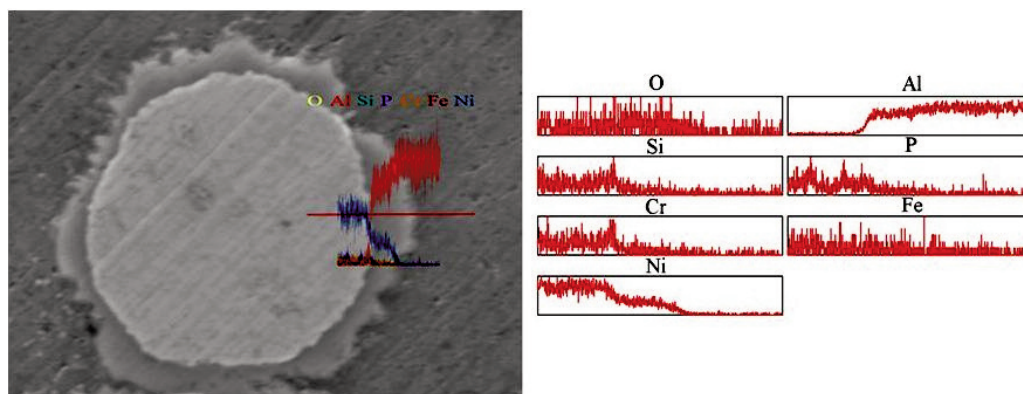


Figure 7. EDS line scanning analysis for hard nickel phase and aluminum matrix

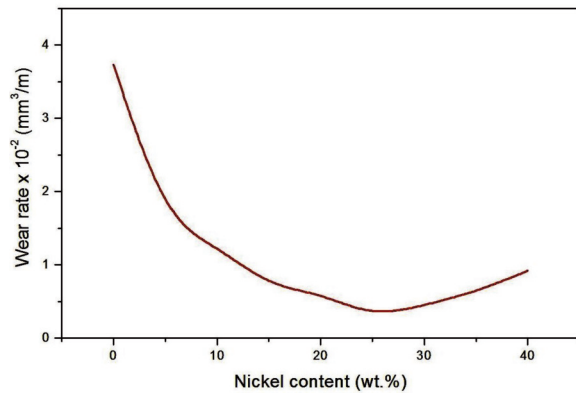


Figure 9. Wear rate versus nickel content

The increase in the wear rate is due to an increase of the intermetallic layer. The material properties change from ductile to fragile characteristics. This trend was also observed in the friction coefficient examinations shown in Figure 10. The contact stress between the counterface and composite has a maximum value at the first stage of sliding during the wear test. The contact surface increases gradually with increasing sliding distance and the contact pressure drops and reaches a steady-state value. For all samples, the steady-state condition was reached after 200 m of sliding. The produced composite materials exhibited higher wear resistance than pure aluminium in all conditions.

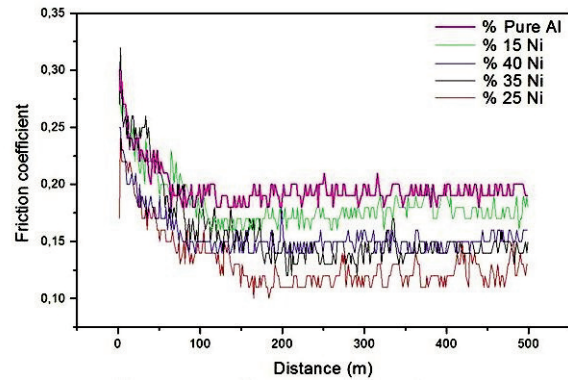


Figure 10. Variation of friction coefficient vs. sliding distance in sintered compacts

This change in the results can be explained by weak bonding formation between the huge amount of reinforcement particles and the aluminium matrix, as presented in the fracture surface images taken by scanning electron microscopy shown in Figure 11. The presence of hard Ni-Al intermetallic particles can also increase the friction coefficient of the material. The main fracture mechanism was determined as ductile for low nickel content. By increasing the nickel content, a clustering of the reinforcement particles occurred and the interface bonding was easily destroyed, causing intergranular fracture, as clearly shown in Figure 11d. For this reason, the wear rate and friction coefficient of the samples increased above 25 wt% Ni.

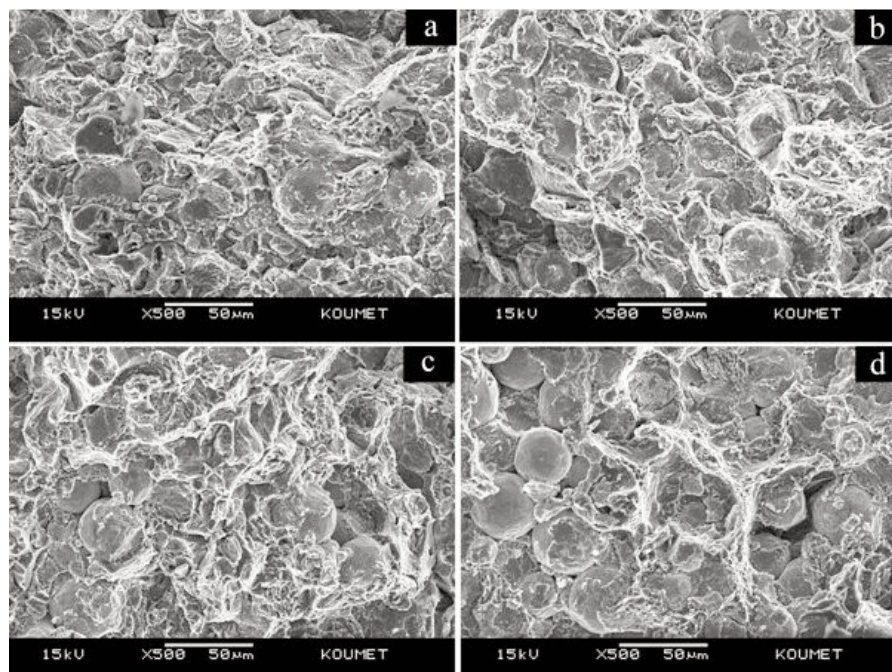


Figure 11. SEM images of fracture surfaces of sintered compacts showing ductile (a-b), ductile and intergranular fracture, a) 15, b) 25, c) 35 and d) 40 wt.% Ni

To understand the wear characteristics of the material, the worn surfaces of the specimens were investigated using SEM. Grooves resulting from micro-cutting are evident in all samples, indicating abrasive wear. The SEM images of the worn surface of the pure aluminium show severe wear, as seen in Figure 12. During the test, oxidation occurs and micro-crack coalescence causes fracture of the oxidised surfaces. The main process can be determined by the transfer of worn material from the centre to the edge, which causes oxidation and fracturing. Large chip formation due to high plastic deformation can be seen clearly in the worn

samples. The worn surfaces became more homogeneous and smoother for the sample with nickel content of 25 wt%, and this sample did not exhibit large chip formation. Plastic deformation was reduced for this nickel content due to the increase in hardness. The wear behaviour of the material became severe abrasive- and delamination-wear at higher nickel-content, showing the same large chip formation on the edge of material due to an increase in the hardness. As a result, from the worn surface examinations, the enhanced wear resistance can be clearly understood by comparing the wear track thickness.

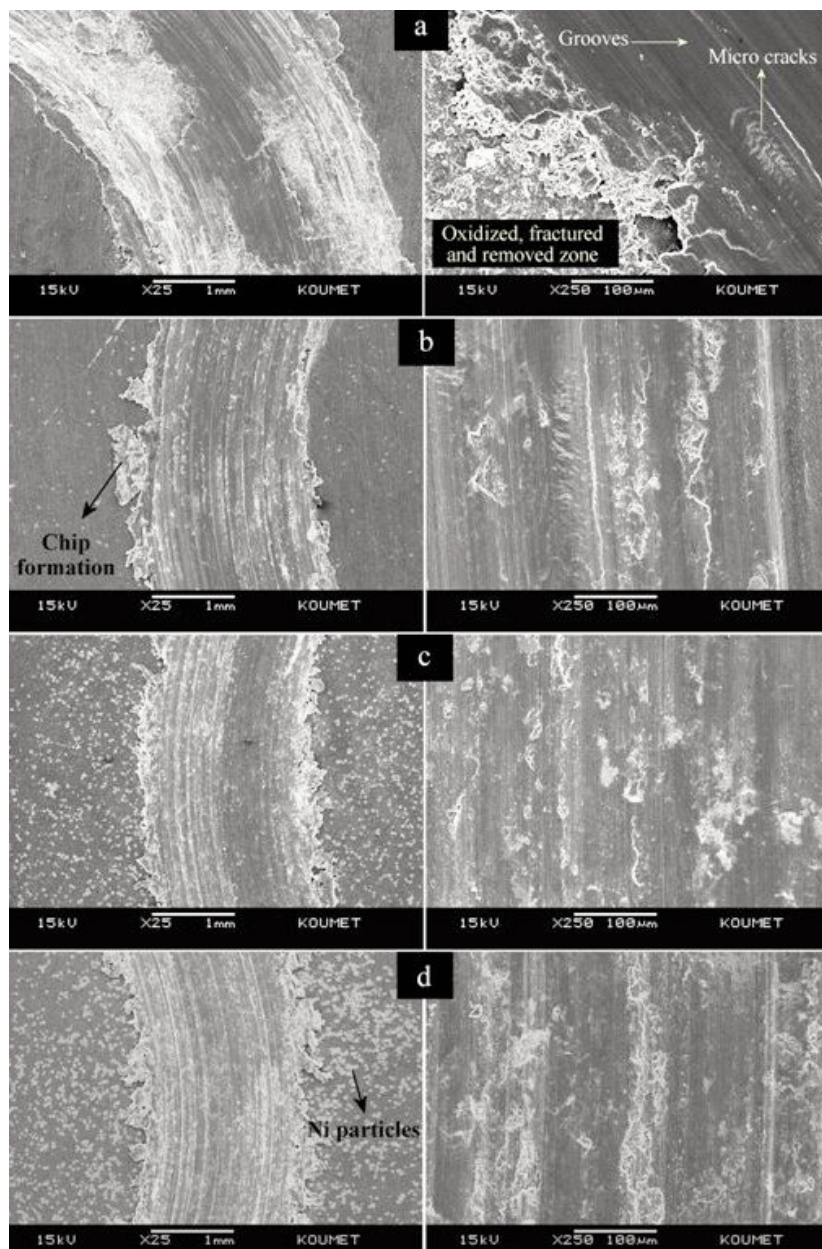


Figure 12. SEM images of worn surfaces of sintered compacts as a function of nickel content, a) pure aluminum, b) 5, c) 25 and d) 35 wt.% Ni

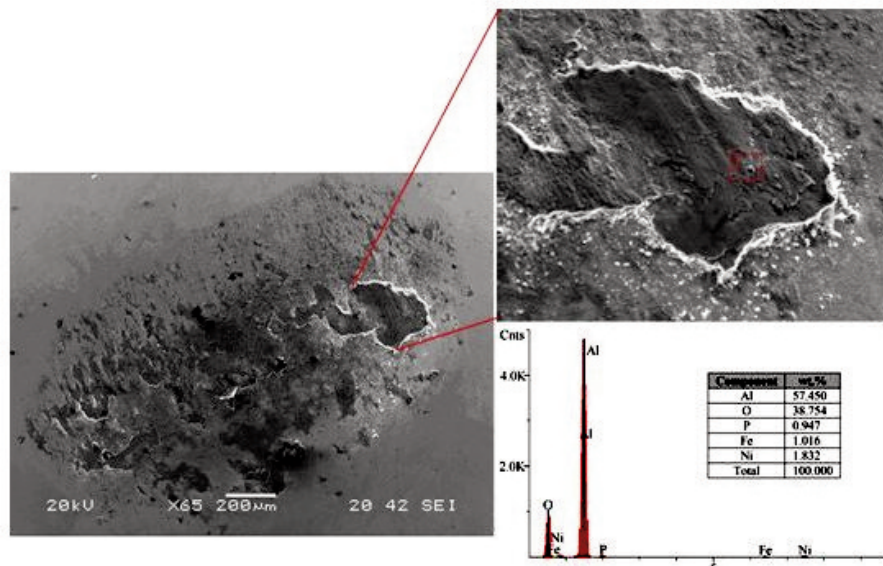


Figure 13. SEM examination of counterface ball after sliding and EDS analysis of adhesive layer transferred from sintered composite

As mentioned before, the main wear mechanism was determined to be abrasive wear. The situation was proved by investigations of the counterface balls using SEM and EDS analysis. An SEM image indicating an adhesion layer from the composite material to the counterface ball and its EDS analysis are presented in Figure 13. It can be seen that aluminium, oxygen, phosphorus, iron and nickel were detected on the counter material that were transferred from the sintered compacts during sliding contact. The high oxygen content proves that oxidation during sliding reduces wear resistance. These results indicate that oxidation wear occurred during the wear tests. This adhesion layer has delaminated from the composite after being plastically deformed underneath the ball.

4. Conclusions

In this study, an in situ metal matrix composite was successfully designed to improve the hardness and wear behaviour of aluminium. The following conclusions are drawn: the reinforcement nickel particles were distributed uniformly in the aluminium matrix. This study demonstrates that nickel particles significantly enhance the hardness and wear properties of aluminium, forming in situ Ni_5Al_3 and Ni_3Al intermetallics. These Ni-Al intermetallic compounds were formed by the diffusion process during hot pressing. The hardness of the material increased with increasing nickel reinforcement content inside the matrix. However, the wear resistance of aluminium decreased when the reinforcement content exceeded a critical value, due to reinforcement clustering. This clustering prevents

the formation of strong bonding, causing intergranular fracture. The predominant wear mechanisms are abrasive, oxidation and delamination wear. The optimum nickel content was determined as 25 wt% nickel content. The hardness of material increased considerably above this nickel content but showed brittle characteristic.

Acknowledgements

This study was supported by the Scientific Projects Unit of Kocaeli University. The author would like to express his gratitude to Senten-BIR A. S. (Izmir, Turkey).

References

- [1] F. Bardi, M. Cabibbo, E. Evangelista, S. Spigarelli, M. Vukcevic, *Mat Sci Eng A-Struct.*, 339 (2003) 43-52.
- [2] S. Kumar, V. Balasubramanian, *Tribol Int.*, 43 (2010) 414-422.
- [3] R. Yamanoglu, M. Zeren, *RM German, J Min Metall Sect B-Metall.*, 48 (2012) 73-79.
- [4] S. Zor, M. Zeren, H. Ozkazanc, E. Karakulak, *Anti-Corros Method M.*, 57 (2010) 185-191.
- [5] R. Rosliza, WB Wan Nik, HB. Senin, *Mater Chem Phys.*, 107 (2008) 281-288.
- [6] J. Adamiec, *AMSE*, 28 (2007) 333-336.
- [7] M. Krasnowski, T. Kulik, *Intermetallics*, 15 (2007) 1377-1383.
- [8] P. Veronesi, R. Rosa, E. Colombini, C. Leonelli, G. Poli, AJ. Casagrande, *J Microwave Power EE.*, 44 (2010) 46-56.
- [9] TB. Massalski, JL. Murray, KH. Bennet, H. Baker, *Phase Diagrams*, American Society for Metals, Metals Park OH 1986.

- [10] P. La, M. Bai, Q. Xue, W. Liu, *Surf Coat Tech.*, 113 (1999) 44-51.
- [11] SK. Pradhan, SK. Chanda, P. Bose, M. De, *Mater Chem Phys.*, 68 (2001) 166-174.
- [12] K. Morsi, *Mat Sci Eng A-Struct.*, 299 (2001) 1-15.
- [13] S. Cheng, G. Yang, J. Wang, C. Yang, M. Zhu, YJ. Zhou, *J Mater Sci.*, 44 (2009) 3420-3427.
- [14] HY. Lee, JK. Roe, A. Ikenaga, *Wear* 260 (2006) 83-89.
- [15] PA. Ikenaga, Y. Goto, Y. Nitta, M. Kawamoto, K. Kobayashi, KJ. Uenishi, *Jpn. Foundry Eng. Soc.*, 68 (1996) 417-422.
- [16] J. Meng, C. Jia, QJ. He, *J Alloy Compd.*, 421 (2006) 200-203.
- [17] JG. Barriocanal, P. Perez, G. Garces, P. Adeva, *Intermetallics* 14 (2006) 456-463.
- [18] R. Arroyave, D. Shin, ZK. Liu, *Acta Mater.*, 53 (2005) 1809-1819.
- [19] R. Venkatesh, *Mat Sci Eng A-Struct.*, 268 (1999) 47-54.